INTERNATIONAL JOURNAL FOR NUMERICAL METHODS IN ENGINEERING
Int. J. Numer. Meth. Engng 2007; **69**:2058–2074
Published online 31 July 2006 in Wiley InterScience (www.interscience.wiley.com). DOI: 10.1002/nme.1833

FEM and BEM coupling in elastostatics using localized Lagrange multipliers

José A. González[1,*,†], K. C. Park[2,‡] and Carlos A. Felippa[2,§]

[1]*Escuela Superior de Ingenieros, Avda. de los Descubrimientos s/n, E-41092 Sevilla, Spain*
[2]*Department of Aerospace Engineering Sciences, Center for Aerospace Structures, University of Colorado, Boulder, CO 80309-0429, U.S.A.*

SUMMARY

The equations produced by the finite and boundary element methods in structural mechanics are expressed in different variables and cannot be linked without modifications. Conventional coupling methods of these numerical techniques have traditionally been based on the use of classical Lagrange multipliers making a direct connection of the two solids through their common interfaces using matching meshes and altering the formulation of one of the methods to make it compatible with the other. In this work, a discrete surface called *frame* is interposed between the connected subdomains to approximate their common interface displacements, it is treated using a finite element discretization and connected to each substructure using localized Lagrange multipliers collocated at the interface nodes. This methodology facilitates the connection of non-matching finite and boundary element meshes avoiding modifications to the numerical methods used and providing a partitioned formulation, which preserves software modularity.

Received 31 January 2006; Revised 26 May 2006; Accepted 9 June 2006

KEY WORDS: finite element method; boundary element method; coupling; localized Lagrange multipliers

1. INTRODUCTION

The finite element method (FEM) and the boundary element method (BEM) are well-known and established numerical techniques used for solving a wide range of engineering problems. Both techniques coexist as effective design tools because they have their own range of applications; the

*Correspondence to: José A. González, Escuela Superior de Ingenieros, Avda. de los Descubrimientos s/n, E-41092 Sevilla, Spain.
†E-mail: japerez@us.es
‡E-mail: kcpark@titan.colorado.edu
§E-mail: carlos@titan.Colorado.EDU

Contract/grant sponsor: Ministerio de Ciencia y Tecnología, Spain; contract/grant number: DPI2003-00487

BEM is well suited, for example, to treat homogeneous infinite domains with linear constitutive models or regions of high stress concentration and the FEM is preferred when dealing with heterogeneities or constitutive non-linearities.

As a proving of this are the efforts dedicated by many researchers to incorporate advantages of one of these two methods into the other. Some examples are the treatment of infinite or semi-infinite regions using boundary-type finite elements like the ones proposed by Felippa [1, 2] and Peters *et al.* [3], or the works by Bonnet *et al*. [4] and Vodička *et al*. [5] developing the symmetric Galerkin BEM, a BE formulation that leads to symmetric and indefinite linear systems.

The main difficulty when mixing the FEM and the BEM is that the system of equations produced by these two methods are expressed in different variables and cannot be linked without modifications. That is the reason why many coupling techniques have been proposed trying to alter the formulation of one method to make it compatible with the other, and finally combine their advantages. An extensive literature survey on this topic can be found in Reference [6].

The first BEM–FEM coupling formulations were proposed in the pioneering works of Zienkiewicz *et al*. [7, 8] and Brebbia and Georgiou [9] that formulated the coupling problem using two different points of view; the first one considers the BE region as a FE region, forcing a symmetrization of the BE substructure on the basis of energy error minimization considerations; and the second one tries to reformulate the FE region to make it compatible with the BE equations.

Later, many applications and improvements of these coupling techniques appeared, like the work of Guarracino *et al*. [10] where a formulation to model and solve the classical soil–structure interaction problem was developed based on coupling Somigliana's equation in discretized form for the elastic half-space with the system, which comes from the FE approximation of the structure. They used a suitable fundamental solution and an appropriate discretization in order to obtain a symmetric and positive definite system matrix, which enables a very simple coupling with matrices coming from the structure. However, their symmetrical BE formulation is restricted to the half-space case, making a node to node connection between the half-space and a structural frame modelled using beam elements.

Other coupling methods soon appeared in many other fields, for example, Frangi [11] in fracture mechanics and Belytschko and Lu [12] in structural and soil dynamics, proposed a new variational formulation for FEM–BEM coupling in elastodynamics using a combined variational principle with test functions that have to be continuous through the BE–FE interface. In time-harmonic elastodynamic problems, Galan and Abascal [13, 14] used a variational approach to couple BEM and FEM domains with coincident meshes at their common interfaces and Cloteau *et al.* [15], Lie *et al*. [16] and Soares *et al.* [17] dedicated their efforts to study the numerical stability and proposed different iterative resolution strategies to solve dynamical problems.

However, there are not many contributions considering the coupling between the FEM and the BEM when dealing with non-matching meshes. The first attempts to provide more general coupling procedures in elasticity started with the works of Hsiao *et al*. [18, 19] and Schnack and Türke [20]. The essential feature of their coupling procedure is the use of a generalized compatibility condition which allows to relax the continuity requirements for the displacement field. In particular, the mesh points of the BE region can be chosen independently of the nodes of the FE structure so that various independent meshes can be connected via mortar-like elements on the interface. Following the same idea, Fisher and Gaul [21] proposed a formulation to solve coupled acoustical fluid–structure problems using mortar-like methods, where coupling is done using classical Lagrange multipliers and the mortar method imposing a continuity condition at the interface. These formulations are quite effective but tend to generate monolithic schemes that do not preserve software modularity.

DOI: 10.1002/nme

In this work, a coupling formulation based on the use of localized Lagrange multipliers is proposed using a discrete surface or *frame* interposed between the subdomains to approximate their interface displacements. This *frame* is treated with a FE discretization that is connected to the BE or FE substructures using localized Lagrange multipliers collocated at the structural interface nodes. This methodology is an extension of the formulation proposed by Park and Felippa [22, 23] to connect non-matching FE meshes.

Compared with other formulations, our proposal facilitates the connection of non-matching FE and BE meshes providing a partitioned formulation which preserves software modularity and can satisfy exactly a constant stress transmission through the interface when a proper discretization of the *frame* is used [24].

2. LOCALIZED FORMULATION OF A COUPLED BEM–FEM SYSTEM

Let us consider two subdomains connected through their common interface Γ_{int}, the first one is denoted Ω^{BEM} and will be modelled by the BEM and the second one is Ω^{FEM} to be treated using the FEM. The interface mesh of Γ_{int} is located between both subdomains and assumed to be non-matching as illustrated in Figure 1. A key approach of the present localized formulation is to treat the non-matching interfaces by the method of localized Lagrange multipliers that yields a symmetric form of the interface constraint operators and can utilize modular BEM and FEM analysis modules. Specifically, instead of a direct coupling of the interface forces between these two subdomains, we will introduce an auxiliary surface or *frame* between them and consider the coupling in terms of interactions of our two solids with this new surface. This procedure is illustrated in Figure 1.

When the model is generated via a symmetric formulation, to evaluate the energy of the system one can apply the variational-based formulation proposed by Park *et al.* [22, 23, 25]. As a majority of BEM models are constructed via non-symmetric formulations, we will employ instead a virtual work approach, thus utilizing a BEM analyser module as a stand-alone package. To this end, the virtual work variation of the total system $\delta\Pi^{\text{total}}$ consists of those of the FE substructure

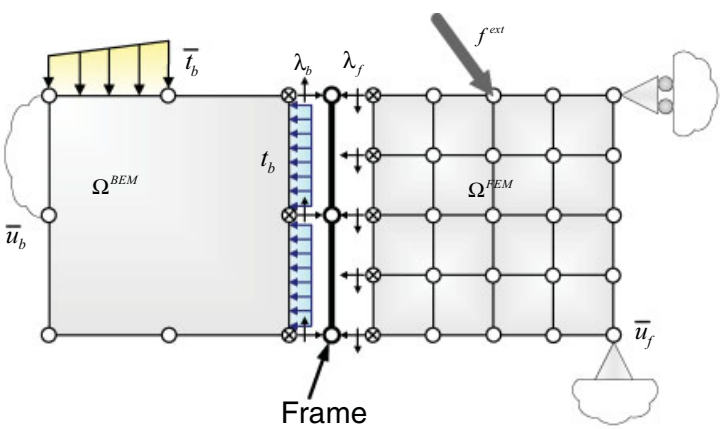

Figure 1. Exploded view of the boundary element (left) and finite element (right) subdomains connected by the frame.

DOI: 10.1002/nme

$\delta\pi^{\text{FEM}}$, of the BEM structure $\delta\pi^{\text{BEM}}$, plus of the interface frame $\delta\pi^{\text{frame}}$; decomposition that can be written as

$$\delta\Pi^{\text{total}} = \delta\pi^{\text{FEM}} + \delta\pi^{\text{BEM}} + \delta\pi^{\text{frame}} \tag{1}$$

The virtual work for the interface frame $\delta\pi^{\text{frame}}$ enforces the kinematical positioning of the frame in a weak sense with the following expression:

$$\delta\pi^{\text{frame}} = \int_{\Gamma_{\text{int}}} \delta\{\lambda_{bi}(v_i - u_{bi})\}\,\mathrm{d}\Gamma_{\text{int}} + \int_{\Gamma_{\text{int}}} \delta\{\lambda_{fi}(v_i - u_{fi})\}\,\mathrm{d}\Gamma_{\text{int}} \tag{2}$$

where both integrals are extended to the boundary interface Γ_{int}, the localized Lagrange multipliers and the boundary displacements (λ_{bi}, u_{bi}) are defined for the BE side, the same couple is defined for the FE side (λ_{fi}, u_{fi}) and the frame displacements are represented by v_i.

We now summarize the virtual work of each one of these three components: the BEM structure, the FEM structure and the interface frame.

3. VIRTUAL WORK OF STRUCTURES MODELLED BY THE BOUNDARY ELEMENT METHOD

The BEM formulation for elastic continua is well known and can be found in many classical texts like Reference [26], where a boundary integral equation for a domain Ω with boundary Γ is obtained by substitution of the fundamental solution into the *Maxwell–Betti* equation of elasticity, a particularization of the *second Green identity* for elastostatics, that can be written as

$$\int_\Gamma t_{bj}\Psi_j\,\mathrm{d}\Gamma + \int_\Omega \rho b_j \Psi_j\,\mathrm{d}\Omega = \int_\Gamma t_j^\Psi u_{bj}\,\mathrm{d}\Gamma + \int_\Omega \rho b_j^\Psi u_{bj}\,\mathrm{d}\Omega \tag{3}$$

where Ψ_j are the weighting functions, t_{bj} are the components of the boundary tractions, u_{bj} are the components of the boundary displacements and b_j are the internal forces.

Equation (3) when using as weighting functions the fundamental solution tensors for displacements $U_{ij}(\mathbf{y}, \mathbf{x})$ and tractions $T_{ij}(\mathbf{y}, \mathbf{x})$ in elastostatics, solution of Navier's equation at $\mathbf{x}$ in the ith direction due to a unit load applied at $\mathbf{y}$ in the jth direction inside an infinite domain, provides a new expression called the *Somigliana identity*, that can be written as

$$c_{ij}(\mathbf{y})u_{bj}(\mathbf{y}) + \int_\Gamma u_{bj}(\mathbf{x})T_{ij}(\mathbf{y}, \mathbf{x})\,\mathrm{d}\Gamma(\mathbf{x}) = \int_\Gamma t_{bj}(\mathbf{x})U_{ij}(\mathbf{y}, \mathbf{x})\,\mathrm{d}\Gamma(\mathbf{x}) + \int_\Omega \rho b_j U_{ij}(\mathbf{y}, \mathbf{x})\,\mathrm{d}\Omega \tag{4}$$

where $c_{ij}(\mathbf{y})$ is the local tensor at point $\mathbf{y}$, with $c_{ij}(\mathbf{y}) = \frac{1}{2}\delta_{ij}$ for smooth boundary points and $c_{ij}(\mathbf{y}) = \delta_{ij}$ for internal points (an explicit analytic expression of the local tensor $c_{ij}(\mathbf{y})$ for other configurations is available in the literature as well). Expressions for the fundamental solution tensors in elastostatics can also be found in Reference [26].

To formulate the BEM, we consider a three-dimensional domain Ω^{BEM} with boundary Γ^{BEM} that is divided into n_{be} discrete elements

$$\Gamma^{\text{BEM}} = \bigcup_{j=1}^{n_{be}} \Gamma_j \tag{5}$$

DOI: 10.1002/nme

where for each element Γ_j, the field of boundary tractions and displacements will be approached using its nodal values.

The number of nodes n_{ne} of a boundary element depends on the desired approximation; in this work we have used isoparametrical quadrilateral and triangular linear elements. Using vector notation, displacements and tractions inside the boundary element j can be approached in the following way:

$$\mathbf{u}_b(\xi_1, \xi_2) = \mathbf{N}_b(\xi_1, \xi_2)\mathbf{u}_b^j; \quad \mathbf{t}_b(\xi_1, \xi_2) = \mathbf{N}_b(\xi_1, \xi_2)\mathbf{t}_b^j \tag{6}$$

where $\mathbf{u}_b(\xi_1, \xi_2)$ and $\mathbf{t}_b(\xi_1, \xi_2)$ are the approximated distributions of displacements and tractions as a function of the element natural co-ordinates (ξ_1, ξ_2), $\mathbf{u}_b^j$ and $\mathbf{t}_b^j$ are vectors with dimension $3n_{ne} \times 1$ containing the nodal values of element j and

$$\mathbf{N}_b(\xi_1, \xi_2) = \begin{bmatrix} N_1 & 0 & 0 & \cdots & N_{n_{ne}} & 0 & 0 \\ 0 & N_1 & 0 & \cdots & 0 & N_{n_{ne}} & 0 \\ 0 & 0 & N_1 & \cdots & 0 & 0 & N_{n_{ne}} \end{bmatrix} \tag{7}$$

is the BE shape functions approximation matrix with dimensions $3 \times 3n_{ne}$ where $N_i(\xi_1, \xi_2)$ is the shape function associated with node i.

The same shape functions used for the variables are used to discretize the geometry, approaching the boundary element surface in the following way:

$$\mathbf{x}(\xi_1, \xi_2) = \sum_{i=1}^{n_{ne}} N_i(\xi_1, \xi_2)\mathbf{x}_i \tag{8}$$

where $\mathbf{x}_i$ are its nodal co-ordinates.

After the discretization process, in the absence of internal forces $b_j = 0$, Equation (4) evaluated at nodal positions becomes

$$\mathbf{c}_i\mathbf{u}_{bi} + \sum_{j=1}^{n_{be}} \mathbf{H}_{ij}\mathbf{u}_b^j = \sum_{j=1}^{n_{be}} \mathbf{G}_{ij}\mathbf{t}_b^j \tag{9}$$

where

$$\mathbf{H}_{ij} = \int_{\Gamma_j} \mathbf{T}\mathbf{N}_b \, \mathrm{d}\Gamma_j = \int\int \mathbf{T}\mathbf{N}_b \mathscr{J} \, \mathrm{d}\xi_1 \, \mathrm{d}\xi_2 \tag{10}$$

$$\mathbf{G}_{ij} = \int_{\Gamma_j} \mathbf{U}\mathbf{N}_b \, \mathrm{d}\Gamma_j = \int\int \mathbf{U}\mathbf{N}_b \mathscr{J} \, \mathrm{d}\xi_1 \, \mathrm{d}\xi_2 \tag{11}$$

are integrals over element j when the collocation point matches with node i, $\mathscr{J} = |\partial\mathbf{x}/\partial\xi_1 \times \partial\mathbf{x}/\partial\xi_2|$ is the Jacobian of the transformation from the real geometry to the natural co-ordinates (ξ_1, ξ_2) in accordance with the geometry approximation given by Equation (8) and the *fundamental solution* tensors (U_{ij}, T_{ij}) are ordered using two 3×3 matrices named $\mathbf{U}$ and $\mathbf{T}$.

These integrals over Γ_j can be easily computed when the collocation points are located outside the element j using a standard Gauss numerical quadrature. However, when the collocation point i belongs to the integration element j, the kernels $\mathbf{U}$ and $\mathbf{T}$ contain singularities of type $O(1/r)$

DOI: 10.1002/nme

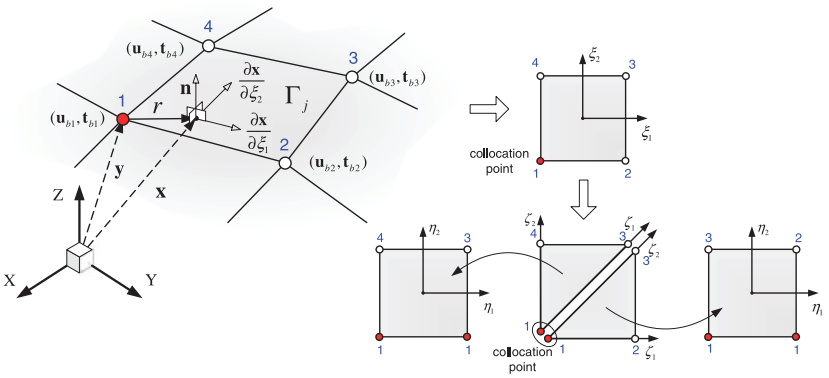

Figure 2. Scheme for local integration over a quadrilateral boundary element by its reduction to triangles.

and $O(1/r^2)$, respectively, being r the distance to the collocation point. For this situation, see Figure 2, the integration domain Γ_j is subdivided into triangles and subsequent transformation of these triangles into squares yields a Jacobian of type $O(r)$ which cancels out the singularity and allows again the use of standard Gauss integration quadrature to evaluate $\mathbf{G}_{ij}$. The computation of the integrals $\mathbf{H}_{ij}$ containing a strong singularity is avoided by using the zero traction condition under rigid body motion. More details of this integration process can be found in Reference [27].

Finally, expression (9) can be applied for all the boundary nodes to yield the final system of equations in matrix form

$$\mathbf{H}\mathbf{u}_b - \mathbf{G}\mathbf{t}_b = \mathbf{b} \tag{12}$$

where vector $\mathbf{b}$ contains all boundary conditions multiplied by corresponding columns of matrix (10) or (11).

In order to cast the above BEM equation in terms of a complementary virtual work, we invoke an idea akin to d'Alembert's principle where the boundary displacement term $\mathbf{H}\mathbf{u}_b$ is treated as if it is a part of prescribed displacement, just as the inertia force is treated as part of external forces in dynamics, to yield the following complementary virtual work expression:

$$\delta\pi^{\mathrm{BEM}} = \delta\mathbf{t}_b^{\mathrm{T}}\{\mathbf{H}\mathbf{u}_b - \mathbf{G}\mathbf{t}_b - \mathbf{b}\} \tag{13}$$

where the boundary tractions vector $\mathbf{t}_b$ includes not only the tractions from the external boundaries, but also the tractions of the interface. This vector could then be decomposed into two different parts: $\mathbf{t}_{b0}$ containing the tractions corresponding to the external boundaries and $\mathbf{t}_{b\lambda}$ containing the interface tractions, i.e. $\mathbf{t}_b^{\mathrm{T}} = \{\mathbf{t}_{b0}, \mathbf{t}_{b\lambda}\}^{\mathrm{T}}$. To simplify notation, in the following we will refer only to the interface tractions $\mathbf{t}_{b\lambda}$ writing them as $\mathbf{t}_b$ and omitting any differentiation (introducing $\mathbf{t}_{b0}$ in the final coupling formulation will be straightforward).

It should be also noted that the above expression does not represent variation of a potential energy functional and that for symmetric Galerkin BEM models will be slightly different due to the fact that the Somigliana traction and displacement identities are of different nature (one representing boundary tractions and the other boundary displacements).

DOI: 10.1002/nme

4. VIRTUAL WORK OF STRUCTURES MODELLED BY THE FINITE ELEMENT METHOD

To formulate the virtual work of the FEM structures, we consider a three-dimensional domain Ω^{FEM} that is divided into n_{fe} finite elements

$$\Omega^{\text{FEM}} = \bigcup_{e=1}^{n_{fe}} \Omega_e \tag{14}$$

and write the potential energy of this elastic substructure in terms of contribution of each finite element Ω_e, obtaining

$$\pi_e^{\text{FEM}} = \frac{1}{2}\int_{\Omega_e} \boldsymbol{\sigma}^{\text{T}}\boldsymbol{\varepsilon}\,\mathrm{d}\Omega_e - \int_{\Omega_e} \mathbf{u}_f^{\text{T}}\mathbf{b}\,\mathrm{d}\Omega_e - \int_{\Gamma_e} \mathbf{u}_f^{\text{T}}\bar{\mathbf{t}}\,\mathrm{d}\Gamma_e \tag{15}$$

where terms due to the elastic strain energy and contributions from volume forces $\mathbf{b}$ and boundary tractions $\bar{\mathbf{t}}$ can be identified.

We use solid isoparametrical elements and the classical FEM formulation, approaching in Ω_e the element displacement field u_f using its nodal values $\mathbf{u}_f^e$ in the following way:

$$\{u_f\} = \mathbf{N}_f \mathbf{u}_f^e \tag{16}$$

where $\mathbf{N}_f$ is the shape functions approximation matrix

$$\mathbf{N}_f(\xi_1, \xi_2, \xi_3) = \begin{bmatrix} N_1 & 0 & 0 & \cdots & N_{n_{ne}} & 0 & 0 \\ 0 & N_1 & 0 & \cdots & 0 & N_{n_{ne}} & 0 \\ 0 & 0 & N_1 & \cdots & 0 & 0 & N_{n_{ne}} \end{bmatrix} \tag{17}$$

and n_{ne} is the number of element nodes.

The strain interpolation can then be expressed $\boldsymbol{\varepsilon} = \mathbf{B}\mathbf{u}_f^e$, where the strain–displacement matrix $\mathbf{B}$ is constructed from the symmetric gradient of (17). The stress interpolation is $\boldsymbol{\sigma} = \mathbf{D}\boldsymbol{\varepsilon}$, where $\mathbf{D}$ collects the constitutive moduli in matrix form.

Substituting these interpolations into (15) produces the variation of the discrete functional for a finite element

$$\delta\pi_e^{\text{FEM}} = \delta\mathbf{u}_f^{e\text{T}}\{\mathbf{K}^e\mathbf{u}_f^e - \mathbf{f}^e\} \tag{18}$$

where $\mathbf{K}^e$ is the element stiffness matrix

$$\mathbf{K}^e = \int_{\Omega^e} \mathbf{B}^{\text{T}}\mathbf{D}\mathbf{B}\,\mathrm{d}\Omega^e \tag{19}$$

and $\mathbf{f}^e$ is the consistent element nodal force vector, given by

$$\mathbf{f}^e = \int_{\Omega^e} \mathbf{N}_f^{\text{T}}\mathbf{b}\,\mathrm{d}\Omega^e + \int_{\Gamma^e} \mathbf{N}_f^{\text{T}}\bar{\mathbf{t}}\,\mathrm{d}\Gamma^e \tag{20}$$

DOI: 10.1002/nme

Considering that the total virtual work of the system can be obtained by adding the contributions from each element, the discrete variational virtual work of the FEM structure is finally expressed as

$$\delta\pi^{\mathrm{FEM}} = \delta\mathbf{u}_f^{\mathrm{T}}\{\mathbf{K}\mathbf{u}_f - \mathbf{f}\} \tag{21}$$

where $\mathbf{K}$ is a symmetric and positive definite matrix constructed from the assembly of element level stiffness matrices (19) and with the vector $\mathbf{f}$ grouping the external forces (20).

Here we should mention again that the FE structural displacements $\mathbf{u}_f$ can be reordered into two different groups: displacements of those nodes that do not belong to the interface $\mathbf{u}_{f0}$ and displacements of the interface nodes $\mathbf{u}_{f\lambda}$. Only the interface nodes will be connected to the frame, using a set of localized multipliers $\boldsymbol{\lambda}_f$ that can be considered as an additional external force applied to the FE substructure. In order to simplify our notation, like it was done previously with the BE partition, we will consider only the interface displacements and refer to them as $\mathbf{u}_f$.

5. VIRTUAL WORK OF FRAMES

The frame is situated between the substructures as illustrated in Figure 3 and its displacements $\mathbf{v}(\xi_1, \xi_2)$ are interpolated using isoparametrical finite elements in the following way:

$$\mathbf{v}(\xi_1, \xi_2) = \mathbf{N}_v(\xi_1, \xi_2)\begin{bmatrix} \mathbf{v}_1 \\ \vdots \\ \mathbf{v}_{n_f} \end{bmatrix} \tag{22}$$

where n_f is the number of nodes in the frame element, $\mathbf{v}_i$ are the nodal displacements, and

$$\mathbf{N}_v(\xi_1, \xi_2) = \begin{bmatrix} N_1 & 0 & 0 & \cdots & N_{n_f} & 0 & 0 \\ 0 & N_1 & 0 & \cdots & 0 & N_{n_f} & 0 \\ 0 & 0 & N_1 & \cdots & 0 & 0 & N_{n_f} \end{bmatrix} \tag{23}$$

is the shape functions approximation matrix.

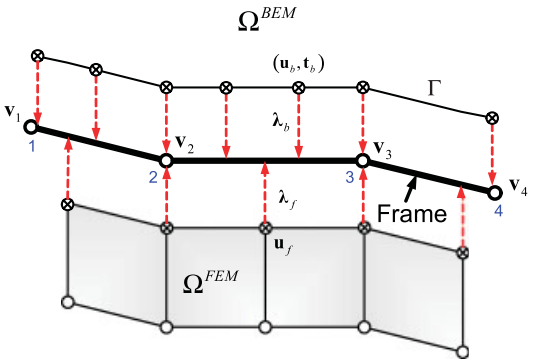

Figure 3. Discretization of the frame displacements and connection with the BE and FE domains.

DOI: 10.1002/nme

Considering the discrete approximations introduced for the variables given by Equations (6), (16) and (22) we can write

$$\{u_b\} = \mathbf{N}_b \mathbf{u}_b, \quad \{t_b\} = \mathbf{N}_b \mathbf{t}_b, \quad \{u_f\} = \mathbf{N}_f \mathbf{u}_f, \quad \{v\} = \mathbf{N}_v \mathbf{v} \tag{24}$$

Next, our choice for the multipliers discretization is to model them as concentrated forces collocated at the subdomain boundary nodes, that is, the interpolations of λ_{bi} for the BEM region and λ_{fi} for the FEM region are *Dirac's* delta functions:

$$\boldsymbol{\lambda}(\xi)_{fi} = \delta(\xi - \xi_f) \cdot \boldsymbol{\lambda}_f, \quad \boldsymbol{\lambda}(\xi)_{bi} = \delta(\xi - \xi_b) \cdot \boldsymbol{\lambda}_b \tag{25}$$

with $\boldsymbol{\xi} = (\xi_1, \xi_2)$ and where $\{\boldsymbol{\xi}_p, p = f, b\}$ are the frame co-ordinates of the substructure node situated at the interface. Exactly the same multipliers approximation was proposed by Park *et al*. [24] to treat the connection of non-matching FEM meshes.

Finally, substitution of (25) into (2) gives the discrete form of the virtual work of the frame as

$$\delta\pi^{\text{frame}} = \delta\{\boldsymbol{\lambda}_b^{\mathrm{T}} \cdot (-\mathbf{u}_b + \mathbf{C}_b \mathbf{v})\} + \delta\{\boldsymbol{\lambda}_f^{\mathrm{T}} \cdot (-\mathbf{u}_f + \mathbf{C}_f \mathbf{v})\} \tag{26}$$

with following definitions:

$$\mathbf{C}_p = \int_{\Gamma_{\text{int}}} \delta(\boldsymbol{\xi} - \boldsymbol{\xi}_p) \mathbf{N}_v \, \mathrm{d}\Gamma_i = \mathbf{N}_v(\boldsymbol{\xi}_p) \quad \Rightarrow \quad \mathbf{C}_b = \mathbf{N}_v(\boldsymbol{\xi}_b), \quad \mathbf{C}_f = \mathbf{N}_v(\boldsymbol{\xi}_f) \tag{27}$$

meaning that $\mathbf{C}_p$ is simply an evaluation of the frame shape functions at the boundary node locations.

6. RELATION OF THE INTERFACE FORCE $\boldsymbol{\lambda}_b$ AND THE TRACTION $\mathbf{t}_b$

It is recalled that the BEM analyser software module possesses its unknown variables in terms of mixed variables, the boundary traction $\mathbf{t}_b$ and the boundary displacement $\mathbf{u}_b$. On the other hand, the virtual work for the frame is expressed in terms of $(\mathbf{u}_b, \boldsymbol{\lambda}_b, \mathbf{u}_f, \boldsymbol{\lambda}_f, \mathbf{v})$. This means one must provide a relation between $\mathbf{t}_b$ and $\boldsymbol{\lambda}_b$.

Of several possibilities, we use a simple *lumping* procedure, see Figure 4, coming from an energy equivalence between the boundary tractions $\mathbf{t}_b$ acting on the boundary element Γ_j and the

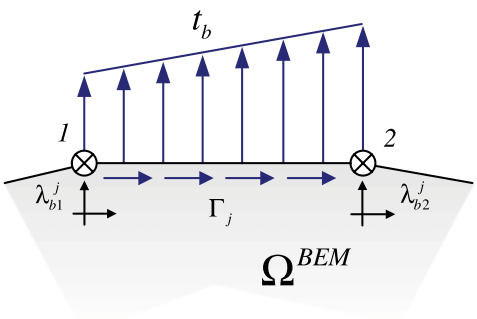

Figure 4. Equivalence between the boundary element tractions and its localized Lagrange multipliers.

DOI: 10.1002/nme

localized multipliers $\boldsymbol{\lambda}_b^j$ acting on its nodes, expressed by the following variational virtual work expression:

$$\delta\pi_j^{\text{lump}} = \int_{\Gamma_j} \delta u_b^{\mathrm{T}} t_b \, \mathrm{d}\Gamma_j - \delta\mathbf{u}_b^{j\mathrm{T}}\boldsymbol{\lambda}_b^j = \delta\mathbf{u}_b^{j\mathrm{T}} \left\{ \left(\int_{\Gamma_j} \mathbf{N}_b^{\mathrm{T}}\mathbf{N}_b \, \mathrm{d}\Gamma_j \right) \mathbf{t}_b^j - \boldsymbol{\lambda}_b^j \right\}$$

$$= \delta\mathbf{u}_b^{j\mathrm{T}} \{\mathbf{M}^j \mathbf{t}_b^j - \boldsymbol{\lambda}_b^j\} \quad \text{with } \mathbf{M}^j = \int_{\Gamma_j} \mathbf{N}_b^{\mathrm{T}}\mathbf{N}_b \, \mathrm{d}\Gamma_j \tag{28}$$

that after its extension to the whole frame can be expressed in matrix form

$$\delta\pi^{\text{lump}} = \delta\mathbf{u}_b^{\mathrm{T}} \cdot \{\mathbf{M}\mathbf{t}_b - \boldsymbol{\lambda}_b\} \tag{29}$$

where $\mathbf{M}$ is the assembling matrix corresponding to the BE interface that transforms boundary tractions into nodal forces.

7. DISCRETE EQUATION FOR COUPLED BEM–FEM SYSTEM

The total virtual work of the coupled BEM–FEM–Frame system can now be expressed from (13), (21), (26), and (29) as

$$\delta\Pi^{\text{total}} = \delta\pi^{\text{BEM}} + \delta\pi^{\text{FEM}} + \delta\pi^{\text{frame}} + \delta\pi^{\text{lump}} \tag{30}$$

which can be expanded to

$$\begin{aligned} \delta\Pi^{\text{total}} = {} & \delta\mathbf{t}_b^{\mathrm{T}}(\mathbf{H}\mathbf{u}_b - \mathbf{G}\mathbf{t}_b - \mathbf{b}) + \delta\mathbf{u}_b^{\mathrm{T}}(\mathbf{M}\mathbf{t}_b - \boldsymbol{\lambda}_b) \\ & + \delta\boldsymbol{\lambda}_b^{\mathrm{T}}(-\mathbf{u}_b + \mathbf{C}_b\mathbf{v}) + \delta\mathbf{u}_f^{\mathrm{T}}(\mathbf{K}\mathbf{u}_f - \boldsymbol{\lambda}_f - \mathbf{f}) \\ & + \delta\boldsymbol{\lambda}_f^{\mathrm{T}}(-\mathbf{u}_f + \mathbf{C}_f\mathbf{v}) + \delta\mathbf{v}^{\mathrm{T}}(\mathbf{C}_b^{\mathrm{T}}\boldsymbol{\lambda}_b + \mathbf{C}_f^{\mathrm{T}}\boldsymbol{\lambda}_f) \end{aligned} \tag{31}$$

The vanishing virtual work of the above expression leads to the following coupled equilibrium equation set:

$$\begin{bmatrix} \mathbf{H} & -\mathbf{G} & \mathbf{0} & \mathbf{0} & \mathbf{0} & \mathbf{0} \\ \mathbf{0} & \mathbf{M} & -\mathbf{I} & \mathbf{0} & \mathbf{0} & \mathbf{0} \\ -\mathbf{I} & \mathbf{0} & \mathbf{0} & \mathbf{0} & \mathbf{0} & \mathbf{C}_b \\ \mathbf{0} & \mathbf{0} & \mathbf{0} & \mathbf{K} & -\mathbf{I} & \mathbf{0} \\ \mathbf{0} & \mathbf{0} & \mathbf{0} & -\mathbf{I} & \mathbf{0} & \mathbf{C}_f \\ \mathbf{0} & \mathbf{0} & \mathbf{C}_b^{\mathrm{T}} & \mathbf{0} & \mathbf{C}_f^{\mathrm{T}} & \mathbf{0} \end{bmatrix} \begin{bmatrix} \mathbf{u}_b \\ \mathbf{t}_b \\ \boldsymbol{\lambda}_b \\ \mathbf{u}_f \\ \boldsymbol{\lambda}_f \\ \mathbf{v} \end{bmatrix} = \begin{bmatrix} \mathbf{b} \\ \mathbf{0} \\ \mathbf{0} \\ \mathbf{f} \\ \mathbf{0} \\ \mathbf{0} \end{bmatrix} \tag{32}$$

where all terms can be easily identified: first equation imposes directly the BEM equations for the BE region, second equation transforms the interface boundary tractions to forces using the

DOI: 10.1002/nme

lumping matrix, third equation imposes compatibility between the BE interface and the frame displacements, fourth equation represents equilibrium for the FE substructure, next expression imposes compatibility between the FE interface and frame displacements and the last one imposes equilibrium on the frame.

It is noted that the resulting coupled system is non-symmetric when the BEM models are generated via Somigliana displacement identity. Finally, the localized multipliers on the BE side can be condensed in order to work only with the natural BEM variables, obtaining the final system

$$\begin{bmatrix} \mathbf{H} & -\mathbf{G} & \mathbf{0} & \mathbf{0} & \mathbf{0} \\ -\mathbf{I} & \mathbf{0} & \mathbf{0} & \mathbf{0} & \mathbf{C}_b \\ \mathbf{0} & \mathbf{0} & \mathbf{K} & -\mathbf{I} & \mathbf{0} \\ \mathbf{0} & \mathbf{0} & -\mathbf{I} & \mathbf{0} & \mathbf{C}_f \\ \mathbf{0} & \mathbf{C}_b^{\mathrm{T}}\mathbf{M} & \mathbf{0} & \mathbf{C}_f^{\mathrm{T}} & \mathbf{0} \end{bmatrix} \begin{bmatrix} \mathbf{u}_b \\ \mathbf{t}_b \\ \mathbf{u}_f \\ \boldsymbol{\lambda}_f \\ \mathbf{v} \end{bmatrix} = \begin{bmatrix} \mathbf{b} \\ \mathbf{0} \\ \mathbf{f} \\ \mathbf{0} \\ \mathbf{0} \end{bmatrix} \tag{33}$$

where a new term $\mathbf{C}_b^{\mathrm{T}}\mathbf{M}$ is used to evaluate the forces on the frame associated with the BE interface tractions.

8. APPLICATIONS

In this section, three representative examples are investigated by solving Equation (32) using direct methods in order to demonstrate the possibilities of the proposed methodology. Eight-node bricks are used in the Ω^{FEM} domains, four-node quadrilaterals are used to discretize the frames and either triangles or quadrilaterals for the boundaries of Ω^{BEM}.

The major objective of these studies is to show the applicability and accuracy of this new coupling approach. Therefore, the results obtained with the FEM–BEM coupled formulation are compared with analytical solutions when possible.

8.1. Uniform tension

The first problem studied is very simple, see Figure 5, a rectangular block with dimensions $B \times B \times 2B$ under a constant stress condition. The block is divided into two identical cubes that are discretized using regular meshes of 150 boundary elements the first one and 64 finite elements the second. These two cubes with non-matching meshes are connected through one of their faces using a planar frame with dimensions $B \times B$.

The material used for the blocks is linear-elastic with constants $E = 13$, $v = 0.3$ and a dimension $B = 1$ is selected. The BEM cube is loaded on the top by a constant traction $\bar{t}_z = 1$ and the vertical displacements are restricted under the FEM block in order to produce a constant σ_z tension field over the solids.

Our intention is to verify that the proposed formulation can reproduce exactly a constant stress transmission through the interface when using a proper discretization for the frame. Conditions to construct the frame mesh are studied by Park *et al*. [24] and named as the *zero moment rule* method. On the right of Figure 5 we reproduce this methodology: *substitute the forces produced*

DOI: 10.1002/nme

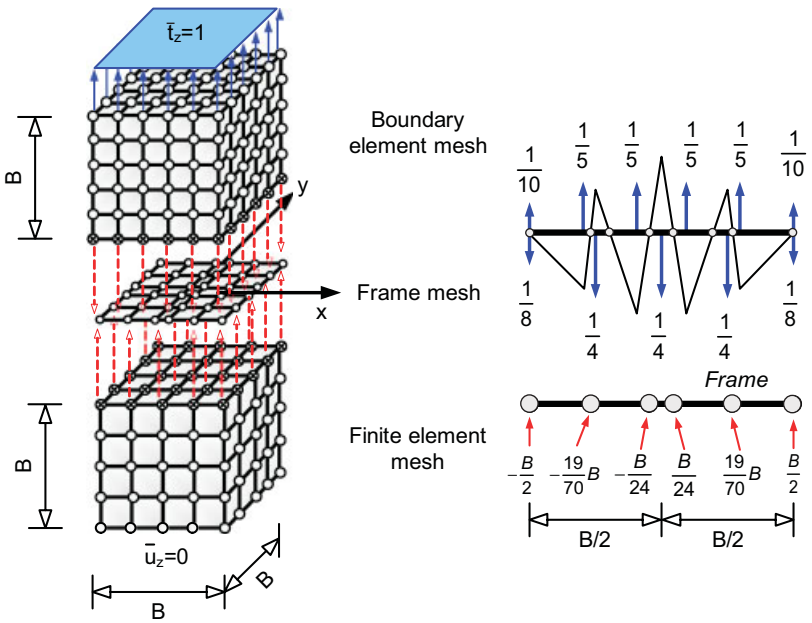

Figure 5. A two-subdomain solid with non-matching FEM and BEM meshes (left) and position of the frame nodes (right).

by the solids on the frame and calculate the moment distribution; *the nodes of the frame have to be situated on the zero moment positions*. Application of this rule gives the eight roots

$$\left\{\frac{-B}{2}; \frac{-19B}{70}; \frac{-B}{5}; \frac{-B}{25}; \frac{B}{25}; \frac{B}{5}; \frac{19B}{70}; \frac{B}{2}\right\} \tag{34}$$

as candidates for frame node locations. If all eight roots are used to construct the frame, the size of some frame elements may be considered too small and it is demonstrated in Reference [24] that frame nodes with roots 2 and 7 can be omitted without numerical problems. Application of this idea results in a frame mesh with 25 elements like the one represented in Figure 5.

The results for this problem are represented in Figure 6 where it can be observed how the exact solution is reproduced, that is, vertical displacement on the top of the block $u_z = 2B\bar{t}_z/E = 0.15385$ and maximal horizontal displacement $u_x = u_y = \nu\bar{t}_z/2E = 0.011538$. It was also verified that an exact constant stress $\sigma_z = 1$ is obtained for all the FE domain and the BE region.

8.2. *Plate in tension with a central hole*

As a classical benchmark, let us consider now the case of stress concentration in a square plate with a central hole due to an uniformly applied external traction. Although this is a plane stress problem, we are going to use a three-dimensional approach in order to test the behaviour of the coupling scheme when combined with curved BEM–FEM interfaces.

DOI: 10.1002/nme

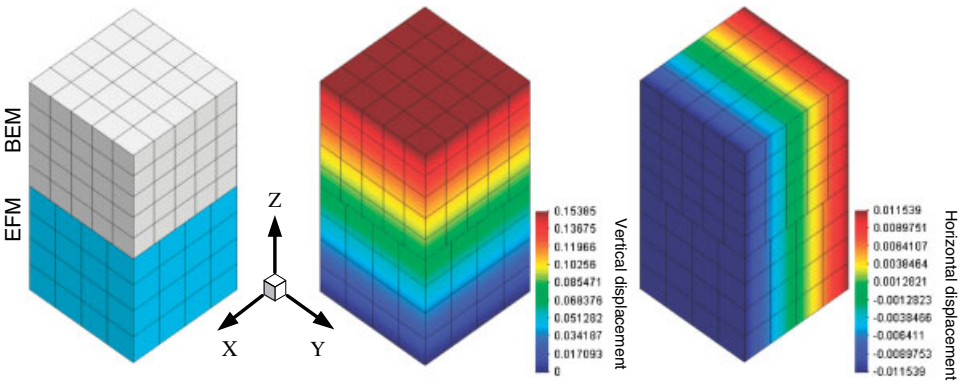

Figure 6. Results for the uniform tension problem. Configuration and displacement contours.

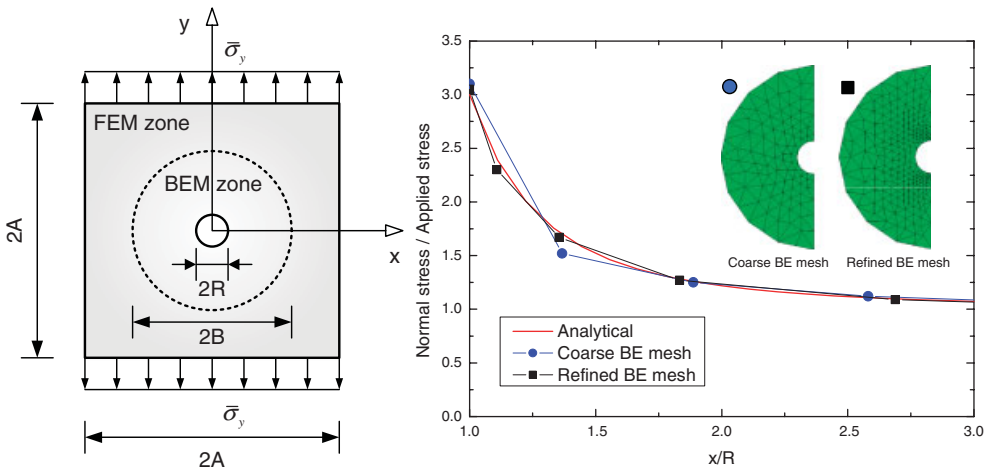

Figure 7. Plate in tension with a central hole (left) and normal stress obtained for two different BE meshes along the x axis (right).

The geometry of the problem is defined in Figure 7 where a constant stress $\bar{\sigma}_y = 100\,\mathrm{kg/cm}$ is applied on a square plate with a side length $A = 9\,\mathrm{cm}$ and a central hole with radius $R = 0.9\,\mathrm{cm}$. A ratio $A/R = 10$ was selected in order to avoid the influence of the finite dimensions of the plate in the stress concentration factor. The plate is supposed to be made of steel with elastic properties $E = 2.1 \times 10^6\,\mathrm{kg/cm^2}$ and $\nu = 0.3$.

To discretize the domain it is first divided into two different zones, the BEM is used around the hole in a circular region of radius $B = 5$ cm and the FEM extends the mesh to complete the domain of the plate. The mesh used for the FEM subdomain contains 32 brick elements and matches with a frame mesh composed of 16 quadrilaterals that connects with a non-matching and more refined BEM mesh used to capture the stress concentration around the hole, see Figure 8.

DOI: 10.1002/nme

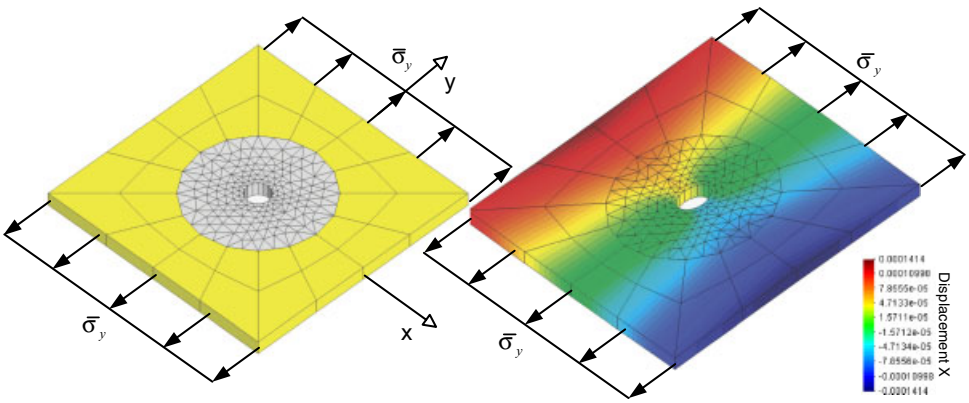

Figure 8. Plate discretization (left) and deformed configuration with horizontal displacement contours (right).

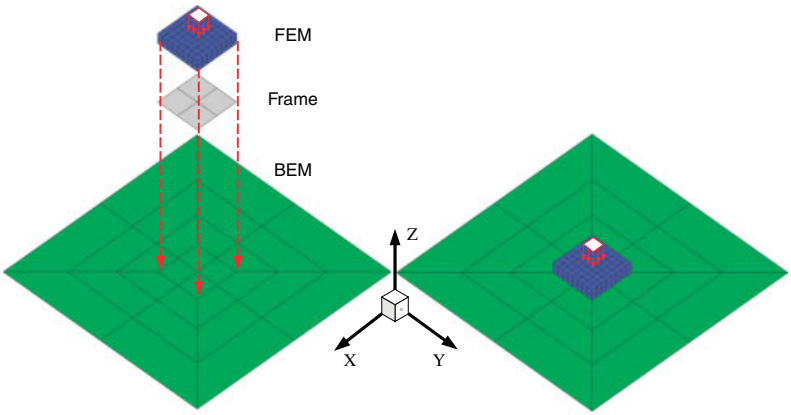

Figure 9. Mesh used for the footing problem. Exploded view (left) and final configuration (right).

To discretize the BEM region two different meshes are used: the first one is a coarse mesh around the hole composed by 740 triangular elements and the second one is a more refined version with 1820 elements. Only one element is used along the plate thickness.

The effect of a central hole in an infinite plate under traction was first investigated by Kirsch in 1898 and later by Savin [28], obtaining the following analytical solution at $y=0$ for the normal stress $\sigma_y(x)$ near the hole:

$$\sigma_y(x) = \frac{\bar{\sigma}_y}{2}\left(2 + \left(\frac{R}{x}\right)^2 + 3\left(\frac{R}{x}\right)^4\right) \quad \text{with } x \geqslant R \tag{35}$$

where the stress concentration effect can be clearly observed when particularized for $x=R$, that is for a point placed at the boundary of the hole, leading to the very well known value of $\sigma_y = 3\bar{\sigma}_y$.

DOI: 10.1002/nme

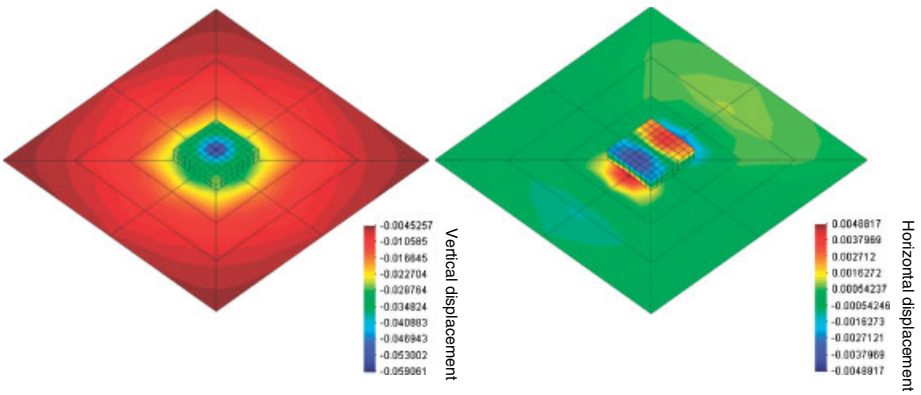

Figure 10. Vertical and horizontal displacements obtained for the footing problem.

The influence of the BE discretization on the normal stresses obtained near the hole is represented in Figure 7 (right) and compared with the analytical solution given by Equation (35). It can be observed that the coarse mesh gives acceptable results, with a 3.3% error in the maximum stress. Much better results are obtained with the finer discretization, that tends correctly to the analytical solution.

8.3. Flexible footing resting on a half-space

The third problem considered is the case of a square shallow foundation with dimensions $2B \times 2B \times 0.5B$ resting on an elastic half-space. The material properties used for the footing are $E_f = 100$, $v_f = 0.3$ and for the half-space $E_b = 10$, $v_b = 0.3$. It is also assumed that the interface between the soil and the structure is perfectly welded, which corresponds to a generalized adhesion condition where tangential tractions remain under the friction limit.

The footing is discretized using a regular mesh of 128 hexahedral finite elements and 243 nodes, see Figure 9, the frame is composed by four quadrilateral elements and the elastic half-space, discretized using a truncated mesh with dimensions $10B \times 10B$, is approximated using 28 quadrilateral boundary elements.

A net vertical load $P = 1$ is applied on the top of the footing, centred and uniformly distributed into four element faces. The numerical results obtained are presented in Figure 10, where the fields of vertical displacements u_z (or settlement) and horizontal displacements u_x are represented.

Although there is no analytical solution for this problem it has been verified that displacements for those points away from the footing tend correctly to the Boussinesq solution.

9. CONCLUSIONS

An accurate, easy to implement and efficient BEM–FEM coupling scheme for three-dimensional elastostatics using localized Lagrange multipliers to connect the substructures to an adaptative interface frame is presented. The algorithm and the introduced formulations prove to be very robust and efficient when solving three-dimensional non-matching coupled problems.

DOI: 10.1002/nme

This BEM–FEM coupling technique is not restricted only to structural problems and can be extended to other fields. In this paper, it has been investigated its application to elastostatics and specially for elastic soil–structure interaction problems, where this technique seems to be very interesting because it gives rise to a real simplification of the problem allowing an easy connection of the structure with the infinite elastic soil.

Suggested methodology simplifies the procedure to solve this kind of problems, minimizing geometrical knowledge needed to couple substructures modelled with different numerical methods. This fact can facilitate further extensions to dynamics and contact problems, work on these subjects by the authors is under way.

REFERENCES

1. Felippa CA. The extended free formulation of finite elements in linear elesticity. *Journal of Applied Mechanics* 1989; **56**:609–616.
2. Felippa CA. A parametric representation of symmetric boundary finite elements. In *Advances in BEM in Japan and U.S.A.*, Tanaka B, Shaw (eds). Computational Mechanics Publications: Southampton, 1990; 365–378.
3. Peters K, Stein E, Wagner WA. New boundary-type finite element for 2D and 3D elastic structures. *International Journal for Numerical Methods in Engineering* 1994; **37**:1009–1025.
4. Bonnet M, Maier G, Polizzotto C. Symmetric Galerkin boundary element method. *Applied Mechanics Review* 1998; **51**:669–704.
5. Vodička R, Mantič V, París F. Symmetric variational formulation of BIE for domain decomposition problems in elasticity—an SGBEM approach for nonconforming discretizations of curved interfaces. *Computer Modeling in Engineering and Sciences* 2005, submitted.
6. State of the art in BEM–FEM coupling. *International Journal of Boundary Element Methods Communication* 1993; **4**(2):58–67.
7. Zienkiewicz OC, Kelly DW, Bettes P. The coupling of the finite element method and boundary solution procedures. *International Journal for Numerical Methods in Engineering* 1977; **11**:355–375.
8. Zienkiewicz OC, Kelly DW, Bettes P. *Energy Methods in Finite Element Analysis* (Chapter Marriage a la mode, the best of both worlds (finite elements and boundary integrals)). Wiley: New York, 1979; 81–106.
9. Brebbia CA, Georgiou P. Combination of boundary and finite elements for elastostatics. *Applied Mathematical Modelling* 1979; **3**:212–220.
10. Guarracino F, Minutolo V, Nunziate L. A simple analysis of soil–structure interaction by BEM–FEM coupling. *Engineering Analysis with Boundary Elements* 1992; **10**:283–289.
11. Frangi A, Novati G. BEM–FEM coupling for 3D fracture mechanics applications. *Computational Mechanics* 2003; **32**:415–422.
12. Belytschko T, Lu YY. A variationally coupled FE–BE method for transient problems. *International Journal for Numerical Methods in Engineering* 1994; **37**:91–105.
13. Galan JM, Abascal R. Numerical simulation of Lamb wave scattering in semi-infinite plates. *International Journal for Numerical Methods in Engineering* 2002; **53**:1145–1173.
14. Galan JM, Abascal R. Elastodynamic guided wave scattering in infinite plates. *International Journal for Numerical Methods in Engineering* 2003; **58**:1091–1118.
15. Clouteau D, Elhabre ML, Aubry D. Periodic BEM and FEM–BEM coupling. Application to seismic behaviour of very long structures. *Computational Mechanics* 2000; **25**:567–577.
16. Lie ST, Yu G, Fan SC. Further improvement to the stability of the coupling BEM–FEM scheme for 2D elastodynamic problems. *Computational Mechanics* 2000; **25**:468–476.
17. Soares Jr D, von Estorff O, Mansur WJ. Iterative coupling of BEM and FEM for nonlinear dynamic analyses. *Computational Mechanics* 2004; **34**:67–73.
18. Hsiao GC, Schnack E, Wendland WL. A hybrid finite-boundary element method in elasticity. *Computer Methods in Applied Mechanics* 1999; **173**:287–316.
19. Hsiao GC, Schnack E, Wendland WL. Hybrid coupled finite-boundary element methods for elliptic systems of second order. *Computer Methods in Applied Mechanics* 2000; **190**:432–485.
20. Schnack E, Türke K. Domain decomposition with BEM and FEM. *International Journal for Numerical Methods in Engineering* 1997; **40**:2593–2610.

DOI: 10.1002/nme

21. Fischer M, Gaul L. Fast FEM–BEM mortar coupling for acoustic-structure interaction. *International Journal for Numerical Methods in Engineering* 2005; **62**:1677–1690.
22. Park KC, Felippa CA. A variational framework for solution method developments in structural mechanics. *Journal of Applied Mechanics* 1998; **65**:242–249.
23. Park KC, Felippa CA. A variational principle for the formulation of partitioned structural systems. *International Journal for Numerical Methods in Engineering* 2000; **47**:395–418.
24. Park KC, Felippa CA, Rebel G. A simple algorithm for localized construction of non-matching structural interfaces. *International Journal for Numerical Methods in Engineering* 2002; **53**:2117–2142.
25. Park KC, Felippa CA, Gumaste UA. A localized version of the method of Lagrange multipliers and its applications. *Computational Mechanics* 2000; **24**:476–490.
26. Brebbia CA, Dominguez J. *Boundary Elements*: *An Introductory Course* (2nd edn). Computational Mechanics Publications: Southampton, 1992.
27. Dominguez J. *Boundary Elements in Dynamics*. Computational Mechanics Publications: Southampton, 1993.
28. Savin GN. *Stress Concentration Around Holes*. Pergamon Press: Tarrytown, NY, 1961.

DOI: 10.1002/nme